Isı Bilimi ve Tekniği Dergisi, 32, 2, 01-09, 2012
J. of Thermal Science and Technology

ISSN 1300-3615

BLAST WAVE SIMULATIONS USING EULER EQUATIONS AND ADAPTIVE GRIDS

Emre ALPMAN
Marmara University, Mechanical Engineering Department,
Göztepe Campus, Kadıköy, Istanbul, Turkey, 34722, emre.alpman@marmara.edu.tr

(Geliş Tarihi :26.08.2010 Kabul Tarihi:03.02.2011)

Abstract: An adaptive grid method which redistributes grid points according to equidistribution principle was implemented to an in-house computational fluid dynamics code capable of simulating blast waves. The resultant code was first tested for a shock tube problem. It was observed that benefit of using adaptive grids becomes more evident when discontinuities in the flow are stronger. It was also observed that interpolation method used to move the flow variables to new grid locations directly affects the accuracy of the solution and interpolation methods which do not guarantee conservation of mass may yield highly inaccurate results. Blast wave simulations performed showed that the adaptive grid method used here improved predictions considerably without requiring a lot of extra CPU time.
Keywords: Blast wave simulations, computational fluid dynamics, adaptive grids, Euler equations, conservative interpolation.

PATLAMA SONRASI OLUŞAN ŞOK DALGALARININ EULER DENKLEMLERİ VE İNTİBAK EDEN ÇÖZÜM AĞLARI KULLANILARAK SİMÜLASYONU

Özet: Çözüm ağı noktalarını eşit-dağılım prensibine göre yeniden dağıtan bir intibak eden ağ metodu, patlama sonrası oluşan şok dalgalarını simule edebilen bir hesaplamalı akışkanlar dinamiği programına uygulanmıştır. Elde edilen program önce bir şok tüpü probleminde denenmiş ve akıştaki süreksizlikler güçlendikçe intibak edici ağları kullanmanın öneminin daha belirgin olduğu gözlemlenmiştir. Ayrıca akış değişkenlerini yeni ağ noktalarına taşıyan interpolasyon metodunun çözümlerin doğruluğunu direk etkilediği ve kütle korunumunu sağlamayan interpolasyon yöntemlerinin oldukça hatalı sonuçlar verdiği görülmüştür. Daha sonar yapılan patlama sonrası oluşan şok dalgası simülasyonları da, uygulanan intibak eden ağ yönteminin sonuçları, harcanan CPU zamanını çok fazla arttırmadan iyileştirdiğini göstermiştir.
Anahtar Kelimeler: Patlama sonrası oluşan şok dalgaları, hesaplamalı akışkanlar dinamiği, intibak eden çözüm ağları, Euler denklemleri, korunumlu imterpolasyon.

NOMENCLATURE

c	Speed of sound [m/s]
C_i	Mass fraction of a species i.
e	Internal energy per unit mass [m^2/s^2]
E	Total energy per unit mass [m^2/s^2]
f	Flux vector of Euler equations
h	Source Vector of Euler equations
H	Total enthalpy per unit mass [m^2/s^2]
N	Number of grid points
p	Static pressure [Pa]
q	Conservative variable vector of Euler equations
r	Physical radial coordinate [m]
t	Time [s]
u	Fluid Velocity [m/s]
w	Weight function
$\dot{w}_i$	Mass production rate of species i
α, β	Weight parameters
ξ	Uniform computational coordinate
ρ	Density[kg/m^3]

INTRODUCTION

An explosion generates high pressure and temperature gases which expand into the surrounding medium to generate a spherical shock wave called a blast wave (Dewey, 2001). Experimental methods to simulate blast waves require handling real explosives. Hence, they may be dangerous and very expensive. On the other hand, computational fluid dynamics (CFD) can be used to generalize and support experimental results in simulating blast waves. Sharma and Long (2001) used Direct Simulation Monte Carlo (DSMC) method to simulate blast waves. DSMC is a very powerful method for detonations and flows with chemical reactions (Long and Anderson, 2000; Anderson and Long, 2002; Anderson and Long, 2003). However, being originally designed for rarefied gas dynamics, it can be very expensive for continuum flows. Also, if one makes a local thermodynamic equilibrium assumption in DSMC, the method becomes equivalent to solving Euler equations (Dewey, 2001). While the entropy after a spherical shock wave decreases radially, the fluid

particles behind it moves isentropically (Dewey, 2001). Therefore, Lagrangian description of fluid flow (White, 2006) becomes very suitable for blast simulation problems. This description was used by Brode (Brode, 1955; 1959) for numerical simulation of blast waves. It is, however, the Eulerian description of the flowfield (White, 2006) that is usually preferred by the many CFD methods (Hoffmann and Chiang, 2004). This description was used in (Alpman, et al. 2007; Alpman, 2009) or blast wave simulations and results showed that Euler equations and Eulerian description of the flow field can be used simulate blast waves and predict blast loads on solid structures (Alpman, et al. 2007; Alpman, 2009; Chen et al. 2007; Chen et al. 2008). A combination of both descriptions for simulating blast waves in one-dimension can be seen in (Smith, 1999).

A blast wave expanding in free-air shows spherical symmetry hence the flowfield can be modeled by one-dimensional Euler Equations written in spherical coordinates. With today's computer power, solution of one-dimensional Euler equations does not require considerable computing time. However, shock waves in the solution domain require very fine grid spacing in the vicinity of them for accurate resolution of high gradients. Since these waves move with time, very fine mesh spacing must be used for the entire flow domain.

Figure 1, also shown in (Alpman, 2009), shows radial pressure distributions obtained from the explosion of 1 kg TNT. The figure clearly shows that there are local steep pressure gradients (shock waves) in the solution domain. However, pressure distribution is very smooth in the other regions of the domain. Since the shock waves are moving, a very fine mesh spacing must be used everywhere even though it may not be required at a given time level. This problem may be overcome by using an adaptive grid technique in which local grid refinement is performed according to the flow gradients in the domain. Hence, fine mesh spacing is only used in the vicinity of the shock waves.

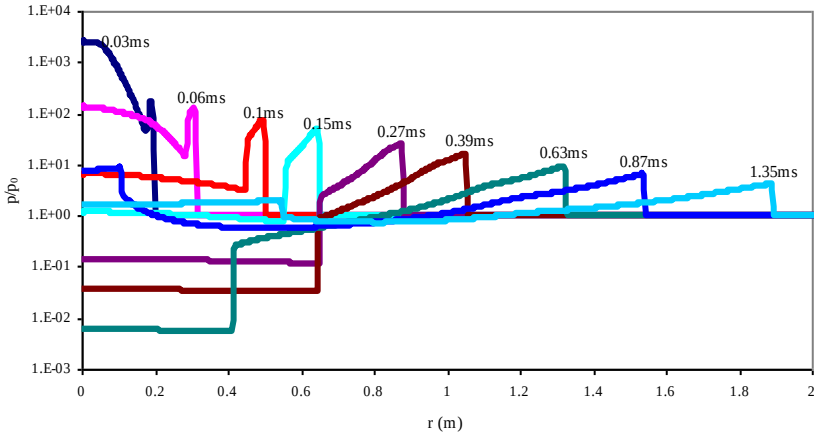

Figure 1. Radial pressure distributions at different times obtained from explosion of 1kg TNT.

The effects of using adaptive grids for numerical solutions has been widely studied and well known. One can find many applications of using adaptive grids for mesh optimization for flows such as separated wakes, boundary layers, and stationary shock waves or contact surfaces. However in the majority of these applications the flowfield is steady. On the other hand, there are few applications for unsteady flows with moving discontinuities. In these flows the grid should be adapted fast enough to follow and resolve the moving discontinuity and also the adopted technique should not increase the computational work excessively. Implementation of such an adaptive grid technique for simulation of flows with strong discontinuities is the aim of the study.

METHODOLOGY

Numerical solutions are performed using an in-house CFD code written by the author in C. The code solves one-dimensional Euler equations in Cartesian, cylindrical, and spherical coordinates. Governing equations were discretized using a second order accurate finite volume technique and the fluxes at cell faces were calculated using the AUSM+ method (Liou, 1996). Second order accuracy was achieved by extrapolating density, velocity and pressure at the cell interfaces. A flux limiter was used to ensure monotonicity (Hoffmann and Chiang, 2004). Resulting semi-discrete equations were solved using a 2 stage modified Runge-Kutta method (Hoffmann and Chiang, 2004). In the solutions, blast wave was generated by explosion of TNT whose effects were introduced to the flowfield as initial conditions. Explosive was modeled as a uniform high pressure sphere where the magnitude of this pressure was obtained using the blast energy released by TNT and the Jones-Wilkins-Lee (JWL) equation of state (Smith, 1999; Dobratz and Crawford, 1985). Although a detonation wave generates non-uniform pressure, density and velocity fields in the explosive (Smith and Hetherington, 1994) the above initial conditions were used for their simplicity.

Blast wave simulation problem involves two different gases; detonation products and surrounding air. Therefore, different state equations for these gases were

required in the solutions. For detonation products, JWL equation of state (Dobratz and Crawford, 1985) was used mainly due to its popularity (Kubota et al. 2007). For surrounding air, calorically perfect gas assumption ceased to be valid because of the temperatures encountered during the simulations (Anderson, 2004). Gas dissociation effects were included by assuming local chemical equilibrium meaning that the chemical reactions occur instantaneously (Hoffmann and Chiang, 2000). Equilibrium relations given in (Tannehill and Mugge, 1974) were used for air to calculate ratio of specific heat capacities and temperature in terms of pressure and density. Temperature of explosion products was obtained by curve fitting to the data given in (Jones and Miller, 1948).

The adaptive grid technique employed in this study redistributes the grid points according to the flow gradients in the domain. The distribution was performed according to equidistribution principle using local flow gradients (van Dam and Zegeling, 2006; Tang and Tang, 2003; Soni et al. 2000; Thornburg et al. 1998). A grid solver was written for this purpose and coupled with the flow solver. Grid generator was called by the solver every 20 time steps and the grid was updated. This way fine mesh spacing was able to be obtained in the vicinity of the shock waves and coarse spacing was able to be used for the other regions of the flow domain.

THEORY

One dimensional Euler equations can be written as follows (Hoffmann et al. 2002):

$$\frac{\partial \mathbf{q}}{\partial t} + \frac{\partial \mathbf{f}}{\partial r} + \mathbf{h} = \mathbf{0} \tag{1}$$

where **q** is the vector containing the conservative variables, **f** is the flux vector, and **h** is the vector containing the source terms:

$$\mathbf{q} = \left[\rho \quad \rho u \quad \rho E\right]^T \tag{2}$$

$$\mathbf{f} = \left[\rho u \quad \rho u^2 + p \quad \rho u H\right]^T \tag{3}$$

$$\mathbf{h} = \frac{n}{r}\left[\rho u \quad \rho u^2 \quad \rho u H\right]^T \tag{4}$$

In the above equations, ρ is the fluid density, u is the fluid velocity, p is the static pressure, E and H are total energy and total enthalpy per unit mass.

$$E = \frac{p}{\rho(\gamma - 1)} + \frac{u^2}{2} \tag{5}$$

$$H = E + \frac{p}{\rho} \tag{6}$$

In equation (5), γ is the ratio of specific heat capacities and in equation (4) $n = 0$ for Cartesian coordinates, $n = 1$ for cylindrical coordinates and $n = 2$ for spherical coordinates.

In this study, equation (1) was discretized using a second order accurate finite volume technique and fluxes at cell faces were calculated using AUSM+ method (Liou, 1996). To ensure monotonicity, Superbee flux limiter was employed.

Explosive Modeling

In this study, a simple model was used for introducing explosion effects to the flowfield. Here, the explosive was modeled as an isobaric high pressure sphere. The solution domain starts from the center of this sphere. Pressure inside this sphere was calculated to be 8.381 GPa, using the JWL equation of state (Dobratz and Crawford, 1985) and the specific explosion energy of TNT. Density of TNT was taken to be 1630 kg/m^3. These are the same conditions used in (Tai et al. 1997) to study underwater explosions. The radius of the high pressure sphere was obtained according to the amount of TNT used. Effects of the explosive were introduced as initial conditions where density and pressure at the grid points lying inside the sphere were initialized to the values given above. Outside the sphere, density and pressure were initialized to 1.225 kg/m^3 and 101320 Pa, respectively. Initial fluid velocity was set to zero for the entire solution domain.

Equation of State for Detonation Products

Two different gases were involved in the solutions; detonation products and surrounding air. These gases were separated by a contact surface which was moving with the local fluid velocity. Different equations of state were used for different sides of this contact surface. As mentioned before, JWL equation of state was used for detonation products (Smith, 1999):

$$p = A\left(1 - \frac{\varpi\,\rho}{R_1\,\rho_0}\right)e^{-R_1\frac{\rho_0}{\rho}} + B\left(1 - \frac{\varpi\,\rho}{R_2\,\rho_0}\right)e^{-R_2\frac{\rho_0}{\rho}} + \varpi\,\rho\,e \tag{7}$$

where e is the specific internal energy and ρ_0 is the initial density of TNT (1630 kg/m^3). Coefficients; A, B, R_1, R_2 and ω are given in (Smith, 1999). Solutions also require calculation of speed of sound. Using thermodynamic relations for perfect gases and equation (7), speed of sound, c, was calculated using equation (8).

$$c^2 = \frac{\frac{p}{\rho^2} - \frac{\partial e}{\partial \rho}}{\frac{\partial e}{\partial p}} \tag{8}$$

ADAPTIVE GRID GENERATION

Adaptive grid technique based on point redistribution was performed using equidistribution principle:

$$wr_\xi = const \tag{9}$$

where r denotes the physical coordinate, ξ denotes the uniform computational coordinate and w is a positive weight function defined using local flow gradients. Subscript means derivative. Differentiating equation (9) in ξ direction yields:

$$\left(wr_\xi\right)_\xi = const \tag{10}$$

Using central differencing, one can approximate equation (10) as:

$$w_{i+1/2}\left(r_{i+1}-r_i\right)-w_{i-1/2}\left(r_i-r_{i-1}\right)=0 \tag{11}$$

where subscripts i, $i\pm1$ denote grid points (cell centers) and $i\pm1/2$ denote mid points (cell faces). Using a Gauss-Seidel-type iteration (Tang and Tang, 2003), new grid points can be obtained using equation (12).

$$\begin{aligned} &w^k{}_{i+1/2}\left(r^k{}_{i+1}-r^{k+1}{}_i\right) \\ &-w^k{}_{i-1/2}\left(r^{k+1}{}_i-r^{k+1}{}_{i-1}\right)=0 \end{aligned} \tag{12}$$

The weight function used in this study was an arc length-type weight function (van Dam and Zegeling, 2006):

$$w=\sqrt{1+\alpha\left(\frac{\partial u}{\partial r}\right)^2+\beta\left(\frac{\partial \rho}{\partial r}\right)^2} \tag{13}$$

Here, derivatives in equation (13) were approximated using central differencing. In equation (13), α and β are user defined weight parameters. Actually this weighting function is problem dependent and requires user input for the parameters. There are more sophisticated functions which require less or no user input in the literature (van Dam and Zegeling, 2006; Soni et al. 2000; Thornburg et al. 1998). However, this function was selected due to its computational simplicity.

Interpolation of Flow Variables

When grid points are redistributed, flow variables must be interpolated to new grid locations. This process can significantly affect the accuracy of the numerical solution. When there are large gradients in the flow field, using typical polynomial or spline interpolation would generate spurious oscillations in the vicinity of shock waves and contact discontinuities. Therefore, a monotone interpolation technique (Fritsch and Carlson, 1980), based on limiting the slopes of flow variables, must be used for such cases. However, although a linear or cubic monotone interpolation (Fritsch and Carlson, 1980) prevents spurious oscillations, it can violate conservation of mass. Therefore, a second order accurate conservative interpolation technique described in (Tang and Tang, 2003) was also used in this study. Unlike in (Tang and Tang, 2003), Superbee limiter (Roe, 1986) was used here to limit the slopes of the flow variables and provide monotonicity.

RESULTS AND DISCUSSION

This section contains the results obtained by the developed code. Numerical solutions were performed on a 1.80 GHz Intel® Core™ 2 Duo processor with 1 GB of memory.

Shock Tube Solution

Since blast wave simulation is basically a moving shock wave problem, developed code was first tested for Sod's shock tube problem (Sod, 1978). In this problem, a stationary high pressure fluid is separated from a stationary low pressure fluid by a barrier. At t = 0 the barrier is removed. This leads to a shock wave and a contact discontinuity move towards the low pressure region and an expansion fan move towards the high pressure region. In this study a shock tube problem with very strong discontinuities was solved using static and adaptive grids and results were compared with the exact solution (Sod, 1978).

The initial conditions were given as follows:

ρ = 1 kg/m^3, u = 0, p = 1x10^5 Pa, $r \le 1$ m

ρ = 0.0001 kg/m^3, u = 0, p = 10 Pa, $r > 1$ m

These were same the conditions studied in (Tai et.al, 1997) as an extremely strong discontinuity case. This case was selected because it more closely resembles a blast wave simulation problem. This problem was solved in Cartesian coordinates, size of the solution domain was 5 m and both fluids were calorically perfect air. Weight parameters α and β were taken as 100 and 20, respectively. Figure 2 shows density predictions obtained using an adaptive grid with N = 126 and three interpolation methods mentioned above. Please note the logarithmic scale used for the vertical axis. From this figure inability of the non-conservative methods to yield accurate solutions is evident. Actually, this was expected because linear and monotone cubic interpolation methods do not guarantee conservation of mass, hence they gravely affected the accuracy of the numerical solution. Conservative interpolation method, however, performed much better compared to others. Therefore, from this point on, only conservative interpolation method will be used in the computations.

Figure 3 displays density distributions obtained using adaptive (N = 126) and static (N = 126 and N = 251) grids. CPU times spent for each solution are shown in Table 1. From this figure, one can clearly see the

improvement made by the adaptive grid when the same number of grid points was used. Of course, adaptive grid solution required more CPU time, however, its predictions were comparable to the static grid solution on twice number of grid points, and in 25% less CPU time. Although adaptive grid technique did not provide much benefit in case 1 where discontinuities were moderate, it really improved the quality of the solution in case 2 where discontinuities were much stronger just as in the case of a blast wave.

Distribution of mesh spacing at t = 1.2 ms along with welocity predictions obtained using adaptive gird were displayed in Figure 4. Note that adaptation was performed according to density and velocity gradients. Examining Figure 4 one can clearly see that the grid points were successfully clustered in locations where gradients were high.

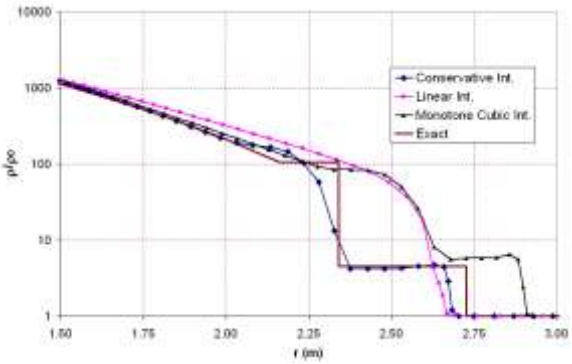

Figure 2. Density distribution at t = 1.2 ms obtained using adaptive grids with different interpolation methods. (ρ_0 = 0.0001 kg/m^3)

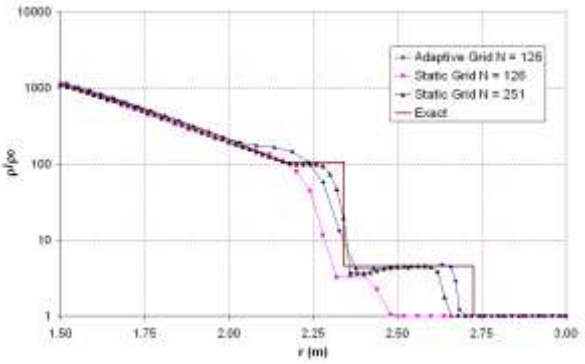

Figure 3. Density distribution at t = 1.2 ms obtained using adaptive and static grids. (ρ_0 = 0.0001 kg/m^3)

Table 1. CPU Times spent for numerical solutions.

	CPU Time
Adaptive Grid (N = 126)	18 sec.
Static Grid (N = 126)	14 sec.
Static Grid (N = 251)	24 sec.

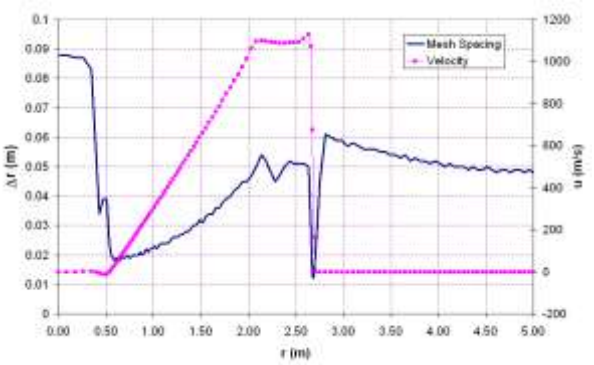

Figure 4. Mesh spacing and velocity distribution at t = 1.2 ms obtained using adaptive grid (N = 126).

Blast Wave Simulation

In this section, blast waves generated from explosion of 1 kg of TNT are displayed. It was assumed that when detonation occurs, explosive material transform the gas phase instantly. Here, the explosive was modeled as an isobaric high pressure sphere in which the density was 1630 kg/m^3 and pressure was 8.381 GPa. Outside this sphere, ambient air density and pressure were 1.225 kg/m^3 and 101320 Pa, respectively. Simulations involved two different fluids; detonation products and ambient air for which different state equations were used. Problem was solved in spherical coordinates and size of the solution domain was 5 m. The weight parameters α and β were taken as 10 and 2, respectively.

One of the important variables in blast wave simulation is the over-pressure, which is the rise of pressure above the ambient pressure downstream of the primary shock wave. Unlike planar shock waves, where shock strength is constant, strength of a spherical shock wave decreases radially (Dewey, 2001).

Figure 5 shows comparison of over-pressure predictions obtained using adaptive (N = 251) and static (N = 251 and N = 500) grids with the data obtained from (Smith and Hetherington, 1994) which states that these results are curve fits to the data used in the weapons effect calculation program CONWEP (Hyde, 1991).

In this figure, r was measured from the explosive center. Numerical solutions mainly over-predicted over-pressure especially at regions close to the explosive. Simple explosive model used here and neglecting any combustion effects that might occur due to detonation were the main reasons for this effect.

However, numerical solutions started to show better agreement with data from (Smith and Hetherington, 1994) as the distance from the explosive increases. Among the three numerical solutions displayed, adaptive grid solution gave the best predictions when r > 1 m.

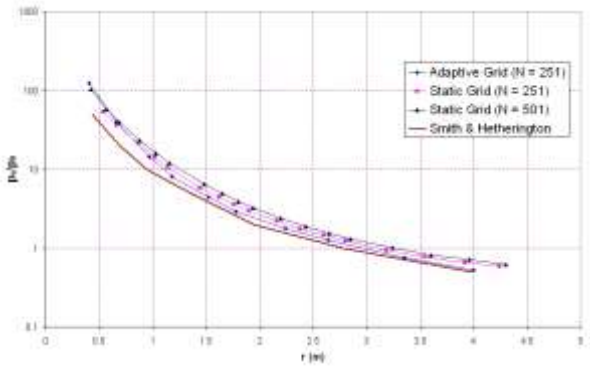

Figure 5. Over-pressure predictions using adaptive (N = 251) and static (N = 251 and N = 501) grids. (p_0 = 101320 Pa)

CPU times spent by the numerical solutions are given in Table 2. Unlike the shock tube problem described in the previous sections, CPU time requirement for adaptive grid solution was only slightly higher than that of static grid solution. This was because of not making calorically perfect gas assumption for the solutions. Actually, here, the code spent considerable time to compute thermodynamic properties of detonation products and high temperature air. Considering the data displayed in Figure 5 and Table 2, one can clearly see the benefit of using adaptive grid for blast wave simulations.

Table 2. CPU Times spent for numerical solutions.

	CPU Time
Adaptive Grid (N = 251)	253 sec.
Static Grid (N = 251)	238 sec.
Static Grid (N = 501)	481 sec.

Figure 6 shows pressure distributions in solution domain at different times obtained using adaptive grid. Here, both the primary and secondary shocks can be visualized. As expected, the secondary shock, which develops after the primary shock, moves away from the explosive for a while. Then, it turns back and moves toward the origin to reflect from the origin. This is typical behavior that had been observed in the previous blast wave simulations (Brode, 1955, 1959; Smith, 1999).

Finally, Figure 7 displays the distribution of mesh spacing at t = 0.2 and 12.4 ms described in Figure 6. It is evident from these figures that mesh was refined only in the vicinity of shock waves and coarse mesh was used everywhere else where the gradients are not high.

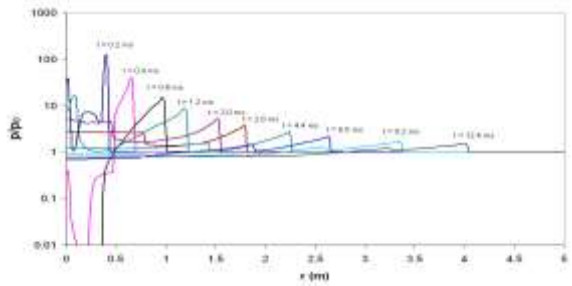

Figure 6. Pressure distribution at different times. (Adaptive grid solution with N = 251).

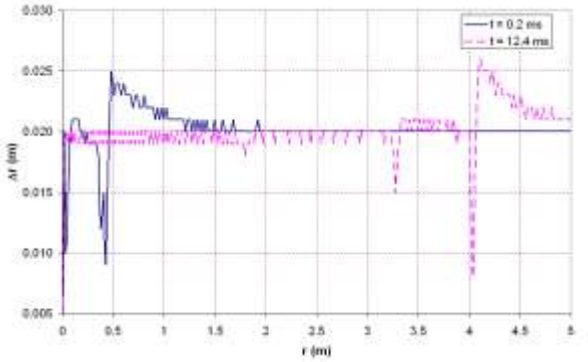

Figure 7. Mesh spacing distribution at t = 0.2 and 12.4 ms (N = 251).

All the blast wave solutions presented above were obtained with the assumption of local chemical equilibrium, meaning that chemical reactions in air occur instantaneously. In order to check the validity of this assumption previous blast wave simulations were repeated including the chemical nonequilibrium effects. This is accomplished by solving additional equations for the mass fractions of reacting species. In this study a five-species, five-reaction chemical model (Hoffman et al. 2002) was used to include nonequilibrium effects. For the forward and backward reaction rates one-temperature model of Park (Park, 1990) was employed. The size of the solution domain was 1 m with N = 51 which resulted in a mesh spacing of 2 cm. Taking mesh spacing as the characteristic length of the flow, the Knudsen number was calculated to be on the order of 10^{-6} around which equilibrium assumption is valid (Hoffman et al. 2002). This resulted in very high reaction rates and made the system of equations very stiff. Figure 8 displays pressure distributions at various times obtained for nonequilibrium (solid line) and equilibrium (dashed line) flows.

Predictions are generally in good agreement except in the vicinity of the secondary shock wave. However, peak pressure predictions are very close to each other which also showed the validity of equilibrium assumption. It is also useful to note that nonequilibrium flow calculations required nearly seven times more CPU time compared to equilibrium flow solution.

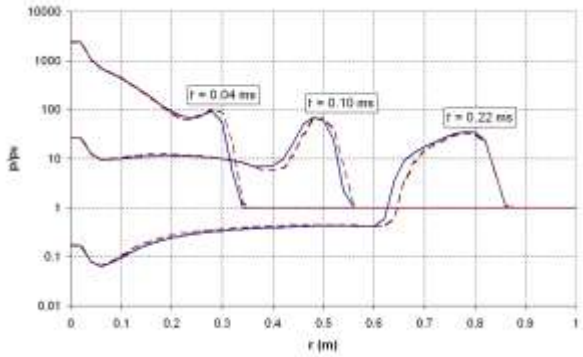

Figure 8. Pressure distributions obtained for nonequilibrium (solid line) and equilibrium (dashed line) flows.

CONCLUSIONS

Simulating shock waves require very fine grid spacing in the vicinity of them for accurate resolution of high gradients. When these waves move, very fine mesh spacing must be used for the entire flow domain if one uses a static grid. Using an adaptive grid, however, only refines the grid where it is necessary and may save considerable computer time and memory. In this work, an adaptive grid technique based on equidistribution principle was implemented to an in-house computational fluid dynamics code, which is capable of simulating moving shock waves. The method used an arc-length type weight function to redistribute the grid points. Three interpolation methods; linear, monotone cubic and conservative, were used to interpolate the flow variables to new grid locations.

Developed code was first tested on planar shock tube problems. Linear and monotone cubic interpolation method yielded inaccurate results due to their lack of ability to conserve mass. Hence, a conservative interpolation method was necessary for accurate predictions. Predictions showed that the benefit of using adaptive grids becomes more evident, when the discontinuities in the flow domain are strong, as in the case of a blast simulation problem.

Over-pressure predictions performed for blast waves due to explosion of 1 kg of TNT showed that using adaptive mesh technique can improve the results without requiring a lot of extra CPU time.

Validity of the equilibrium assumption made for blast wave simulations was also tested by repeating numerical solutions by including chemical nonequilibrium effects. This was achieved by using a five - species, five-reaction chemical model. Pressure predictions obtained for nonequilibrium and equilibrium flows were in good agreement which also reinforced the validity of the equilibrium assumption used in the computations.

REFERENCES

Alpman, E., Long, L, N., Chen, C. –C., Linzell, D. G., Prediction of Blast Loads on a Deformable Steel Plate Using Euler Equations, 1*8th AIAA Computational Fluid Dynamics Conference*, Miami, FL, June 2007.

Alpman E., Simulation of Blast Waves using Euler Equations, *17th National Thermal Science and Technology Conference*, Sivas, Turkey, June 2009. (in Turkish).

Anderson, J. B., Long, L. N., Direct Monte Carlo Simulation of Chemical Reaction Systems: Prediction of Ultrafast Detonations, *Journal of Chemical Physics*, 118 (7), 3102 – 311, 2003.

Anderson, J. B., Long, L. N., Direct Simulation of Pathological Detonations, *18th International Symposium on Rarefied Gas Dynamics*, Vancouver, Canada, 2002.

Anderson, J. D. *Modern Compressible Flow with Historical Perspective*, 3rd Edition, McGraw Hill, 587, 2004.

Brode H. L., Numerical Solutions of Spherical Blast Waves, *Journal of Applied Physics*, 26 (6), 766 – 775, 1955.

Brode, H. L., Blast Wave from a Spherical Charge, *The Physics of Fluids*, 2 (2), 217 – 229, 1959.

Chen, C.C., Alpman, E., Linzell, D.G., and Long, L.N., Effectiveness of advanced coating systems for mitigating blast effects on steel components, *Structures Under Shock and Impact X, Book Series: WIT Transactions on the Build Environment*, 98, 85 - 94, 2008.

Chen, C.C., Linzell, D. G., Long, L. N., Alpman, E., Computational studies of polyurea coated steel plate under blast loads, *9th US National Congress on Computational Mechanics*, San Francisco, CA, July 2007.

Dewey, J. M., Expanding Spherical Shocks (Blast Waves), *Handbook of Shock Waves*, 2, 441 – 481, 2001.

Dobratz, B. M., Crawford, P. C., *LLNL Explosives Handbook – Properties of Chemical Explosives and Explosive Simulants*, Lawrence Livermore National Laboratory, 1985.

Fritsch, F. N., Carlson, R. E., Monotone Piecewise Cubic Interpolation, *SIAM Journal on Numerical Analysis*, 17 (2), 238 – 246, 1980.

Hoffmann, K. A., Chiang, S. T., *Computational Fluid Dynamics for Engineers, Volume I*, Engineering Education System™, 2004.

Hoffmann, K. A., Chiang, S. T., Siddiqui S., Papadakis, M., *Fundamental Equations of Fluid Mechanics*, Engineering Education System™, 2002.

Hoffman, K., A., Chiang, S. T., *Computational Fluid Dynamics, Volume II*, Engineering Education System™, 2000.

Hyde, D. W., *CONWEP: Conventional Weapons Effects Program*, US Army Waterways Experimental Station, 1991.a

Jones, H., Miller, A. R., The Detonation of Solid Explosives: The Equilibrium Conditions in the Detonation Wave-Front and the Adiabatic Expansion of the Products of Detonation, *Proceedings of the Royal Society of London. Series A, Mathematical and Physical Sciences*, 194, 490 – 507, 1948.

Kubota, S., Nagayama, K., Saburi, T., Ogata, Y., State Relations for a Two-Phase Mixture of Reacting explosives and Applications, *Combustion and Flame*, 74 – 84, 2007.

Liou, M. -S., A sequel to AUSM: AUSM+, *Journal of Computational Physics*, 129, 364 – 382, 1996.

Long, L. N, Anderson, J. B., The simulation of Detonations using a Monte Carlo Method, *Rarefied Gas Dynamics Conference*, Sydney, Australia, 2000.

Park, C., *Nonequilibrium Hypersonic Aero-thermodynamics*, John-Wiley & Sons, Inc., 1990.

Roe, P. L., Characteristic-based Schemes for Euler Equations, *Annual Review of Fluid Mechanics*, 18, 337 – 365, 1986.

Sharma, A., Long, L. N., Numerical Simulation of the Blast Impact Problem using the Direct Simulation Monte Carlo (DSMC) Method, *Journal of Computational Physics*, 200, 211 – 237, 2004.

Smith, R. W., AUSM(ALE): A Geometrically conservative Arbitrary Lagrangian-Eulerian Flux Splitting Scheme, *Journal of Computational Physics*, 150, 268 – 286, 1999.

Smith, P. D., Hetherington J. D., *Blast and Ballistic Loading of Structures*, Butterworth-Heinemann, 24 – 62, 1994.

Sod, G. A., A survey of Several Finite Difference Methods for Systems of Nonlinear Hyperbolic Conservation Laws, *Journal of Computational Physics* 27 (1), 1 – 31, 1978.

Soni, B. K., Koomullil, R., Thompson, D. S., Thornburg, H., Solution Adaptive Grid Strategies Based on Point Redistribution, *Computer Methods in Applied Mechanics and Engineering*, 189, 1183 – 1204, 2000.

Tang, H., Tang, T., Adaptive Mesh Methods for One- and Two-Dimensional Hyperbolic Conservation Laws, *SIAM Journal of Numerical Analysis*, 41 (2), 487 – 515, 2003.

Tannehill, J. C., Mugge P. H., Improved Curve Fits for the Thermodynamic Properties Equilibrium Air Suitable for Numerical Computation using Time Dependent and Shock-Capturing Methods, *NASA CR-2470*, 1974.

Tai, C. H., Chiang, D. C., Su, Y. P., Explicit Time Marching Methods for The Time-Dependent Euler Computations, *Journal of Computational Physics*, 130, 191 – 202, 1997.

Thornburg, H., Soni, B. K., Kishore, B., A Structured Grid Based Solution-Adaptive Technique for Complex Separated Flows, *Applied Mathematics and Computation*, 19, 259 – 273, 1998.

Van Dam, A., Zegeling, P. A., A Robust Moving Mesh Finite Volume Method Applied to 1D Hyperbolic Conservation Laws from Magnetohyrdodynamics, *Journal of Computational Physics*, 216, 526 – 546, 2006.

White, F. M., *Fluid Mechanics*, McGraw-Hill, 6th Edition, 17, 2006.

APPENDIX A

Nonequilibrium Flow Equations

Governing equations for nonequilibrium flow was obtained by coupling Euler equations (Eq. 1) with species continuity equation (Hoffmann et al. 2002). For the five-species model used the governing equations become:

$$\frac{\partial \mathbf{q}}{\partial t} + \frac{\partial \mathbf{f}}{\partial r} + \mathbf{h} = \mathbf{w} \tag{A.1}$$

where

$$\mathbf{q} = \begin{bmatrix} \rho & \rho u & \rho E & \rho C_1 & \rho C_2 & \rho C_3 & \rho C_4 \end{bmatrix}^T \tag{A.2}$$

$$\mathbf{f} = \begin{bmatrix} \rho u & \rho u^2 + p & \rho u H & \rho u C_1 & \rho u C_2 & \rho u C_3 & \rho u C_4 \end{bmatrix}^T \tag{A.3}$$

$$\mathbf{h} = \frac{n}{r}\begin{bmatrix} \rho u & \rho u^2 & \rho u H & \rho u C_1 & \rho u C_2 & \rho u C_3 & \rho u C_4 \end{bmatrix}^T \tag{A.4}$$

$$\mathbf{w} = \begin{bmatrix} 0 & 0 & 0 & \dot{w}_1 & \dot{w}_2 & \dot{w}_3 & \dot{w}_4 \end{bmatrix}^T \tag{A.5}$$

Here, C_i is the mass fraction and $\dot{w}_i$ is the rate of mass production of species i (Hoffmann et al. 2002). Conservation of mass requires

$$\sum_{i=1}^{5} C_i = 1 \text{ and } \sum_{i=1}^{5} \dot{w}_i = 0 \qquad \text{(A.6)}$$

The five reactions used in the solutions were as follows:

$$\begin{aligned} N_2 + M &\leftrightarrow 2N + M \\ O_2 + M &\leftrightarrow 2O + M \\ NO + M &\leftrightarrow N + O + M \\ NO + O &\leftrightarrow N + O_2 \\ O + N_2 &\leftrightarrow N + NO \end{aligned} \qquad \text{(A.7)}$$

where M is a species which remains unchanged during the reaction. The forward and backward reaction rates and the corresponding rates of mass productions were calculated using Table 4.14 and Section 4.7.3 of (Hoffmann et al. 2002).

Emre Alpman was born on April 10th, 1977 in Ankara. He completed his high school education in 1995 at the Ankara Gazi Anatolian High School. He attended Aeronautical Engineering Department of Middle East Technical University the in the same year and graduated with the first rank in 1999. After graduation he enrolled to the Master of Science program of Middle East Technical University Aerospace Engineering Department and completed this program in 2001. In 2002 he entered the Pennsylvania State University Aerospace Engineering Department to seek a doctorate degree, which he received in 2006 by graduating from the program. On December 2006 he joined Marmara University Mechanical Engineering Department as an Assistant Professor. Currently, he continues to work in this position.